Geologie en Mijnbouw **70**: 243–252, 1991.

Model calculations on intrusive cooling and related coalification of the Peel-Erkelenz coalfield (The Netherlands and Germany)

Hans Erren* & J.W. Bredewout
*Department of Exploration Geophysics, Institute of Earth Sciences, University of Utrecht, Budapestlaan 4, 3508 TA Utrecht, The Netherlands; * Present address: ITC International Institute for Aerospace Survey and Earth Sciences, Kanaalweg 3, 2628 EB Delft, The Netherlands*

Received 2 October 1990; accepted in revised form 26 February 1991

Key words: coalification, intrusion, kitchening, thermal modeling, Peel-Erkelenz

Abstract

An analytical solution of the simplified heat equation was calculated and applied to a 3D model of the intrusion below the Peel-Erkelenz coalfield. The calculated thermal history was converted to coal ranks with an empirical integral expression. Using a least squares fit of observed coal rank data, an initial temperature of (800 ± 100) °C for the intrusion was obtained. Calculated vertical coal rank gradients are comparable with those observed in the Ibbenbüren coalfield (Bramsche intrusion, FRG).

A detailed 2D finite difference calculation, using the complete heat equation on a 5-layer section in the area, confirmed the analytical results. It also proved that:

1) effects of radiogenic heat production are negligible compared to cooling magma effects;
2) if the coal is remote from the magma, latent heat effects can be simplified by adding 300° C to the initial intrusion temperature;
3) lateral and vertical variations in rock properties have negligible influence on coalification compared to cooling magma effects; a homogeneous model is therefore a good approximation.

Introduction

The Peel-Erkelenz coalfield covers an area of about 450 km^2 in the Dutch province of Limburg and the German state Nordrhein-Westfalen (Fig. 1). It is situated on the Peel-Erkelenz horst, where the Upper Carboniferous Coal Measures (Table 1) are covered by 100–800 m of Cretaceous to Recent deposits.

In the coalfield a strong coal rank anomaly is observed; in the central part of the Sophia-Jacoba concession the anthracite phase, whereas in the same seam on the Dutch part of the area only low volatile bituminous coal is present (Fig. 2). The occurrence of the high temperature/low pressure anthracite ('Edelantrazit') combined with a strong magnetic anomaly of roughly the same extent have been attributed to a mafic intrusion, substantiated by a diabase occurrence in Kamp-Lintfort, which is situated about 50 km north of Erkelenz (Teichmüller & Teichmüller 1966). Bosum (1965) modeled the magnetic anomaly as a wedge-shaped mafic laccolith with a minimum depth of 3 km and a maximum thickness of 11 km (Fig. 3). In the 1980's interest in geothermal energy led to new gravimetric and magnetometric measurements in the area. Gravity stripping on the data, however, yielded a low density for the intrusion, indicating a felsic

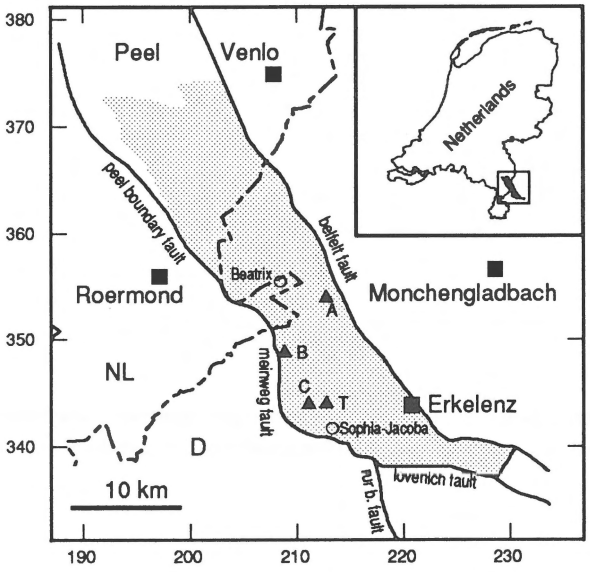

Fig. 1. Location map. Thick lines: faults; dashed line: international boundary; triangles: see text.

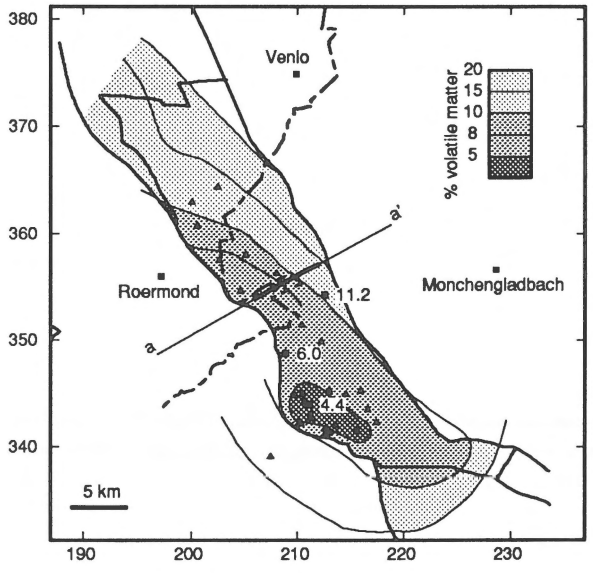

Fig. 2. Contour map of observed coal ranks after Patteisky et al. (1962), Peelcommissie (1963) and Kimpe (1973). Section a-a' see Fig. 8. Triangles indicate selected borehole sites. Numbers are coal rank values of points A B C in Fig. 1.

composition. The slightly elevated geothermal gradient can also be explained by a felsic intrusion (Bredewout 1989).

This study aims to put constraints on the initial temperature of the magma and thus on its composition. A set of thermal histories is calculated from intrusive cooling models with varying parameters. Observed coal ranks are then correlated with these calculated thermal histories using the empirical relationship of Falvey & Deighton (1982). For model calculations on other areas see for example Buntebarth (1985) and Horváth et al. (1986). Software on our calculations is available on request.

Geological setting

An excellent detailed geological study of the German part of the coalfield is published by Wrede (1985). Dutch studies cover the Groot-Beatrix concession (Kimpe 1973) and the Peel area (Peelcommissie 1963, Van Tongeren 1987).

The coalfield is part of the Variscan foredeep which was filled during the Westphalian (Carboniferous) with clastic sediments and organic matter. Rapid subsidence caused an initial coalification (see Table 2), after which the coal measures were folded and uplifted during the Variscan Orogeny. In the present coalfield the intensity of deformation decreases from Southeast (narrow folds and thrusts) to Northwest (no folds). Additional sediments were deposited after the orogeny and to be subsequently eroded during the Jurassic and Early

Table 1. Stratigraphic sequence of the Carboniferous in the Peel-Erkelenz coalfield

Stratigraphic sequence			
	C	> 850 m	
			Ägir
		380 m	
Westphalian	B		*Domina*
		360–400 m	*G.B. 33–45*
			Catharina
		470–480 m	*G.B. 11–32*
	A		*Wasserfall*
		645–530 m	*G.B. 1–10*
			Sarnsbank
Namurian		1050 m	
Dinantian		1200 m	

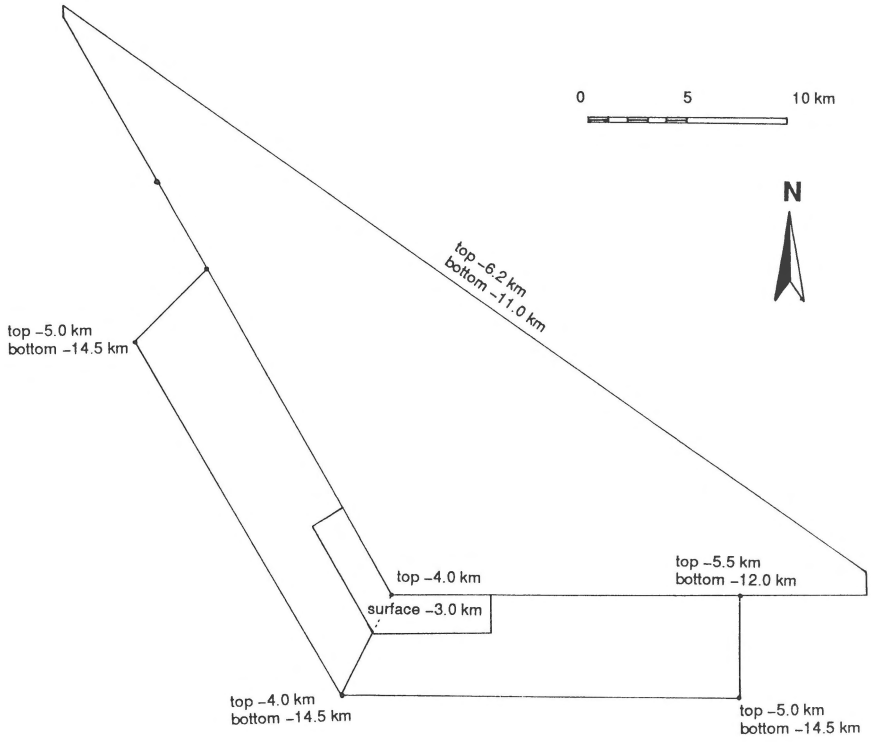

Fig. 3. The intrusion model of Bosum (1965) in plan view. The model is build from four wedge-shaped blocks of which the top and bottom values are given (see also Figs 7 and 8).

Cretaceous. From the Cretaceous onwards sedimentary deposits again covered the coal measures.

The intrusion which is the cause of the magnetic and coal rank anomalies must have had its origin somewhere between the end of the Variscan Orogeny and the beginning of the Cretaceous sedimentation (Patteisky et al. 1962).

Table 2. Initial coal ranks and relative stratigraphic positions (section XII Peelcommissie, 1963). Reflectance values (R_m (0)) are derived from % V.M. in Fig. 5. The Steinknipp (Z) seam is arbitrarily set at 1000 m depth

Seam/Horizon	reflectance	% V.M.	depth (m)
Catharina marine band	1.50	30	530
G.B. 27 Gross Langenberg (E)	1.65	25	630
G.B. 13 Merl (T)	2.00	18	860
G.B. 10 Steinknipp (Z)	2.15	15	1000
G.B. 9 Plasshofsbank	2.25	13	1100
Sarnsbank marine band	2.95	6	1645

Normal faulting as part of a rift zone from the Alps to the North Sea created the Peel-Erkelenz horst in the Tertiary. The horst is bordered in the southwest by the Peel Boundary-Meinweg-Rur Boundary fault system. West of these faults the coal measures are buried deeply. In the northeast the horst is bordered by the Belfeld fault and coal to the east thereof has been removed by erosion.

Theory

Analytical heat conduction

The heat-conduction equation of Fourier for a homogeneous medium, neglecting additional heat production is (Carslaw & Jaeger 1962):

$$\frac{\partial T}{\partial t} = \varkappa \nabla^2 T \qquad (1)$$

where T is temperature, t is time and $\varkappa$ is diffusivity.

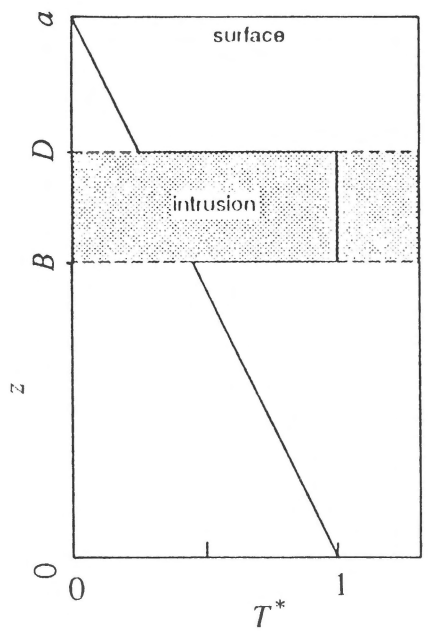

Boundary conditions: $\begin{bmatrix} T^*(t) = 0,\ z = a \\ T^*(t) = 1,\ z = 0 \end{bmatrix}$

Initial conditions : $\begin{bmatrix} T^*(0) = 1,\ B < z < D \\ T^*(0) = 1 - z/a,\ else \end{bmatrix}$

Fig. 4. Boundary and initial conditions (temperature T* vs. depth z). The initial condition is a linear temperature gradient outside the intrusion and a uniform temperature (melting point T* = 1) inside the intrusion (z = B through D).

For the case of the vertical boundary and initial conditions as given in Fig. 4, the solution for a cooling rectangular block with length b, width c and depth reaching from z = B to z = D is (Buntebarth 1984):

$$T^*(x,y,z,t) = 1 - \frac{z}{a} + \sum_{k=1}^{\infty} A_k \sin\frac{k\pi z}{a} \exp\left(-\frac{k^2\pi^2}{a^2}\varkappa t\right) \times \left(\operatorname{erf}\frac{x}{2\sqrt{\varkappa t}} - \operatorname{erf}\frac{x-b/2}{2\sqrt{\varkappa t}}\right) \times \left(\operatorname{erf}\frac{y}{2\sqrt{\varkappa t}} - \operatorname{erf}\frac{y-c/2}{2\sqrt{\varkappa t}}\right) \quad (2)$$

where T* is the temperature $(T - T_{surface})/(T_{melt} - T_{surface})$, and

$$A_k = \left| \frac{2}{k^2\pi^2}\sin k\pi z - \frac{2z}{k\pi}\cos k\pi z \right|_{z=B/a}^{z=D/a} \quad (3)$$

In the 3D modeling case we are dealing with an irregularly shaped body that can be split into a set of stacked rectangular blocks.

Finite difference heat equations

The differential equation describing heat conduction in a static non-homogeneous medium with additional heat production is:

$$\varrho C_p \frac{\partial T}{\partial t} = \nabla \cdot (k \nabla T) + A \quad (4)$$

where ϱ is the density, C_p is the specific heat, T is the temperature, t is the time, k is the thermal conductivity and A is the (radiogenic) heat production.

A two-dimensional geometry (x horizontal, z vertical) results in:

$$\frac{\partial T}{\partial t} = \frac{1}{\varrho C_p}\left(k\frac{\partial^2 T}{\partial x^2} + k\frac{\partial^2 T}{\partial z^2} + \frac{\partial k}{\partial x}\frac{\partial T}{\partial x} + \frac{\partial k}{\partial z}\frac{\partial T}{\partial z} + A\right) \quad (5)$$

Equation (5) was numerically solved in a finite difference mesh following Van den Beukel & Wortel (1986), who also provided the initial FORTRAN software of the Runge-Kutta algorithm by Verwer (1977).

Coalification

To correlate the calculated thermal history with observed coal ranks, the empirical relationship of Falvey & Deighton (1982) was used which relates thermal history to mean vitrinite reflectance R_m.

$$R_m^{\varepsilon}(t_1) = \beta \int_0^{t_1} e^{\alpha T(t)}\, dt + C_0 \quad (6)$$

$\varepsilon = 5.635$, $\beta = 2.7 \times 10^{-6}\,Ma^{-1}$, $\alpha = 0.068\,°C^{-1}$, $C_o = R_m^{\varepsilon}(0)$.

Equation (6) gives a straightforward relationship between coal rank, temperature and time. Also it is easy to convert into a computer algorithm. However, the extrapolation of equation (6) to fast heating at high temperatures may be questionable because the relationship is based on relatively slow heating during burial in a sedimentary basin (Falvey & Deighton 1982).

The initial coal ranks $R_m(0)$ at the start of the calculations are listed in Table 2. They originate from section XII (remote from the intrusion) in Peelcommissie (1963), and are considered a constant for one stratigraphic level.

The observed coal rank data used in this research (Patteisky et al. 1962, Peelcommissie 1963, Kimpe 1973) are more than 15 years old and published as the relative amount of dry and ashfree volatile matter [% V.M.(daf)] (Fig. 2). A graph by Teichmüller & Teichmüller (1984) was used to connect % V.M. of the data set with R_m of equation (6) (see Fig. 5). The samples for Patteisky's coal rank data were taken in the Steinknipp (= Z; Sonnenschein; G.B. 10) reference seam (Table 2), however, some data were extrapolated from more shallow levels to the reference seam with a non-anomalous gradient.

The conversion from % V.M. in R_m introduces an additional inaccuracy. The relationship between mean reflectance and % V.M. is not straightforward for high coal ranks (Teichmüller 1987). The results in the anthracite region ($R_m > 4$), therefore, must be regarded with reservation. Tissot et al. (1987) pointed out that even accurate reflectance measurements can yield different values depending on the laboratory where the measurement has taken place. The limitations of this research, however, did not allow new independent coal petrographic measurements.

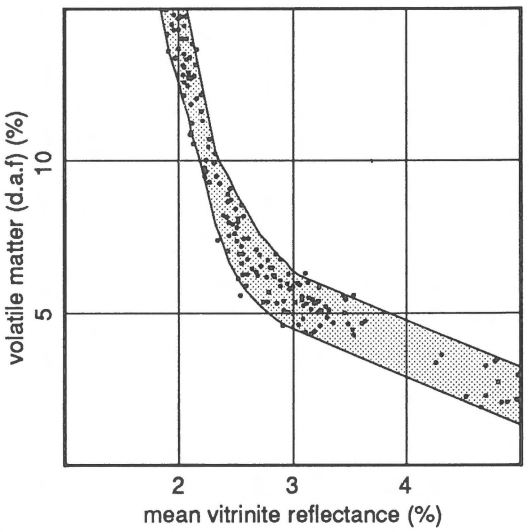

Fig. 5. Relationship between R_m and rate of volatile components (% V.M.), after Teichmüller & Teichmüller, 1984. Grey area: error limit.

Modeling

With the intrusion geometry deduced by Bosum (1965), the thermal history of the area is calculated in two ways: analytically with the simplified heat equation in a homogeneous 3D model, and with a finite difference calculation of the complete heat equation in a layered 2D model (one vertical section of 3D). This 2D calculation was carried out to check if the homogeneous 3D model is not an oversimplification of the problem. For both models thermal history is converted to coal rank (vitrinite reflectance) with equation (6). The model calculations are correlated to published coal rank (volatile matter) observations in Fig. 5.

The area studied is defined by the following edges: The northwestern edge is taken arbitrarily at the southern limit of the Triassic deposits (Peelcommissie 1963). The southwestern edge is the Peel/Rur Boundary fault system. The northeastern edge is the Belfeld fault and the southeastern edge is the Lövenich fault. Outside this area no coal rank data or detailed geologic information were available.

For the model calculations the geology of the area had to be restored to Early Permian geometry. All normal faults were considered to be post Variscan. Although there must have been some normal faulting during the Variscan Orogeny this was neglected in the reconstruction. The reductions were carried out with the stratigraphy at Sophia-Jacoba shaft 1 as levels of reference. The result of the restoring process for the Steinknipp (Z) seam is presented in Fig. 6. The geometry of the cooling intrusion is taken according to the calculations on the magnetic anomaly by Bosum (1965). Due to the car-

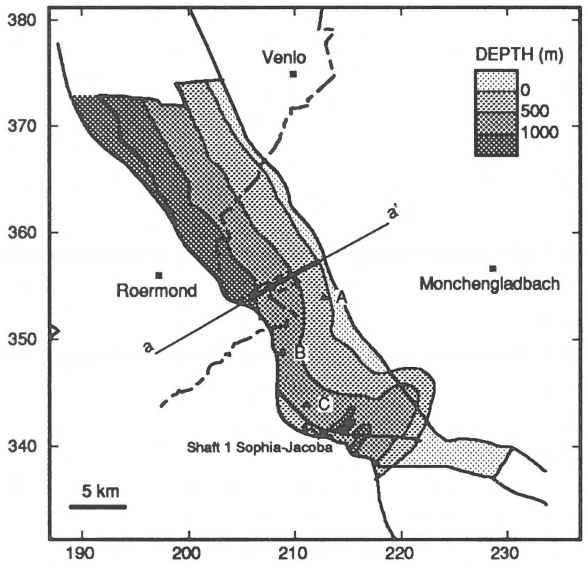

Fig. 6. Contour map of Late Variscan restored depth of seam Steinknipp (Z) (= G.B. 10; Sonnenschein) (see also Fig. 8).

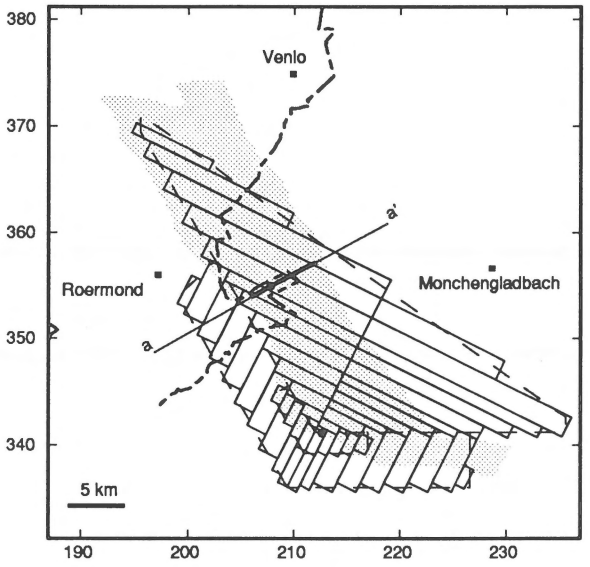

Fig. 7. Intrusion model used for 3D-calculations. Grey: coalfield. Dashed lines: Intrusion boundary of Bosum (1965). Solid lines: outlines of rectangular blocks with different thickness.

tesian limitations of equation (2), Bosum's model was cut into a set of rectangular blocks (Figs 7 and 3).

The equations were written into a FORTRAN program. For all blocks the temperature anomalies were calculated and summed. The time integration concerned a time span of only 3 Ma: due to the exponential relationship of equation (6) the low temperature tail of the temperature history makes no significant contribution to the calculation of the coal rank. Three gauge points situated in the Steinknipp (Z) seam, but in different lateral positions (A, B, C Figs 1 and 6) were used to calculate the best fit by varying the parameters that govern the equations, the additional sediment thickness, the initial intrusion temperature, the background heat flow and the diffusion parameter. The reason for taking only three points lies in the amount of computing involved for varying the above parameters. With the optimum parameters the kitchening effect is calculated for all borehole locations of Wrede (1985), Kimpe (1973) and Peelcommissie (1963) in the coalfield.

Several authors (Carslaw & Jaeger 1962, Giberti et al. 1984, Buntebarth 1985) have considered that latent heat can be taken into account by adding about 300° C to the real melting temperature, this 300° C being the quotient of the latent heat and the specific heat L/C_p. The benefit of this is that the calculations simplify drastically as both L and C_p are a function of temperature.

In the finite difference 2D calculations a 5 layer model was constructed containing section III of Kimpe (1973) (see Fig. 8). A mesh interval distance of 500 m was chosen. Values for C_p and k are given in Table 3 (Haenel 1983). Heat production due to radioactive decay was taken according to Table 4 (Haenel 1983) and a base heat flow at the bottom line of the section of 88.5 mW m^{-2} was adopted. Heat production caused by friction was neglected. Latent heat was corrected for in two ways: firstly by a gradual release of heat in the magma (see Giberti et al. 1984), secondly by increasing the initial intrusion temperature. In the coal region of the model there was no difference noticeable. The second method was more economic with computing time, so it was adopted in the rest of the 2D modeling.

Results

For the 3D modeling a least-squares fit provides the best agreement between calculated and observ-

ed coalification at the 3 gauge points. The maximum temperature in the coal seam depends greatly on the thickness of the sediment layer that covered the intrusion during cooling. In Fig. 9 the results are plotted for the parameters that have the strongest influence on the results: the additional sedimentary cover, the initial model temperature and the equilibrium geothermal gradient. The best fit is obtained for an initial model temperature of about 1100° C. This temperature corresponds – after correcting for latent heat effects by subtracting a traditional 300° C – with an initial intrusion temperature of (800 ± 100) °C. This rather low temperature agrees better with a felsic than with a mafic magma.

In order to obtain a more detailed picture of the coal rank distribution of the Steinknipp (Z) seam, the results of the least-squares fit were used in a calculation on all borehole sites of Wrede (1985), Kimpe (1973) and Peelcommissie (1963). A map is presented in Fig. 10. In Fig. 11 the misfit of the calculations vs. the observations is plotted for this model; only a few calculations deviate. For a seam higher in the stratigraphy (the Groß Langenberg, E or G.B. 27 seam, see Table 2) the coal rank was also calculated for the total area and a coal rank gradient map was constructed (Fig. 12). If these calculated gradients are compared with actually observed coal rank gradients in the Bramsche intrusive halo (Ibbenbüren coalfield, FRG) (Teichmüller & Teichmüller 1985) it appears that they are in agreement (calculated Peel-Erkelenz: 1.25%/370 m vs. observed Ibbenbüren: 0.38%/100 m). The maximum temperature was calculated for one horizontal level before faulting (Fig. 13). Fluid inclusion measurements (Bredewout 1989) on a rock sample taken in point T of Fig. 1 point to a maximum rock temperature of at least 204° C, which is not in contradiction with our results.

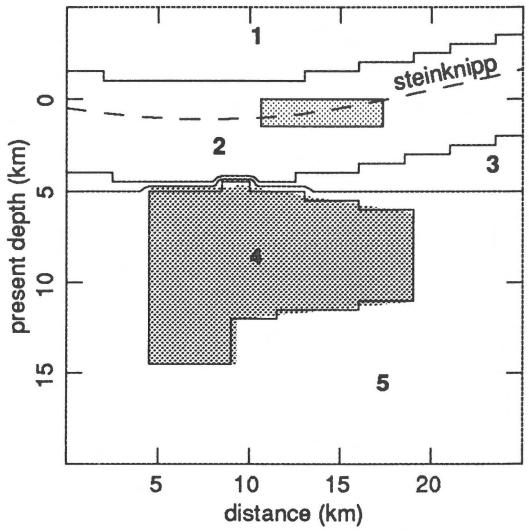

Fig. 8. Section a-a′ (see Figs 2, 6 & 7). Model used for 2D finite difference calculations. 1 Additional sedimentary cover; 2 Carboniferous; 3 Devonian; 4 Magma; 5 Upper crust. Shaded box: Geological section III in Kimpe (1973). Dark grey: Magnetic body of Bosum (1965).

For the 2D finite difference calculations the 500 m mesh interval proved to be too coarse to get extra information. However, confirmation of the 3D results was obtained. Two solutions are shown in Fig. 14: A high intrusion temperature combined with a thin sedimentary cover and a low intrusion temperature with a thicker sedimentary cover. Both give about the same agreement between data and calculations. This lack of discrimination can be due to the relatively small contribution of the intrusion to the total coalification at this location. In addition we found that:

Table 3. Values for thermal conductivity k, specific heat C_p and density ϱ (Haenel 1983)

Material	k (W m^{-1} K^{-1})	C_p (J m^{-1} K^{-1})	ϱ (kg m^{-3})
Carboniferous	3.09	871	2680
Devonian	2.83	840	2590
upper crust	2.10	840	2670
magma	2.10	840	2700

Table 4. Heat production rates (A) of rocks (Haenel 1983). See also equation (2.1)

Material	A (μW m^{-3})
sediment	1.13
upper crust	$5.5 \times e^{(-z/9400)}$
felsic magma	3.00
mafic magma	1.55

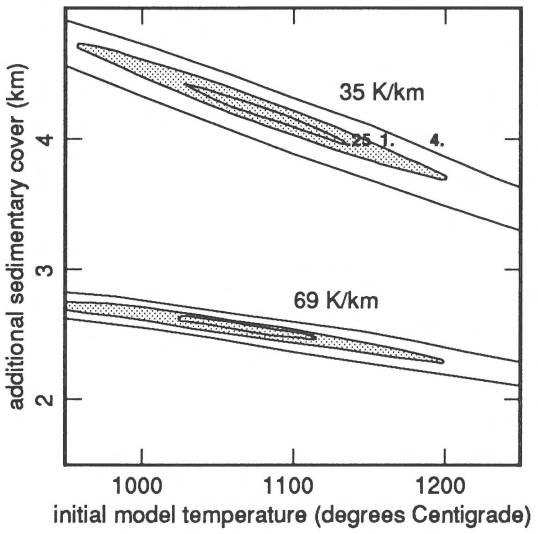

Fig. 9. Contour graph of least squares errors of 3D-calculations for a geothermal gradient of 35° C/km (top) and of 69° C/km (bottom).

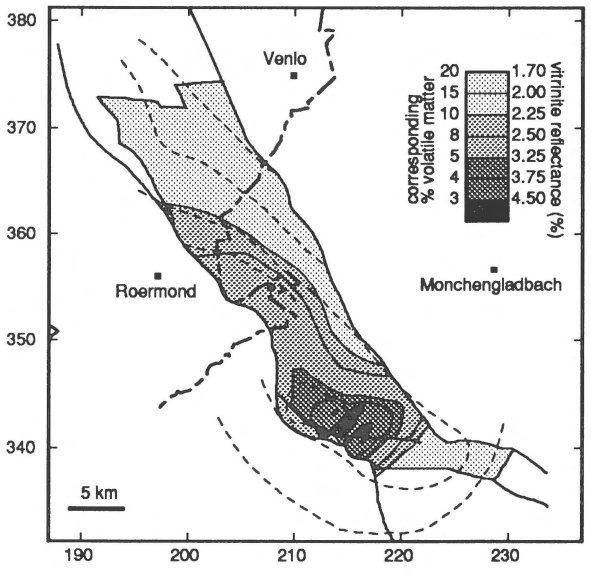

Fig. 10. Contour map of calculated vitrinite reflectance for seam Steinknipp (Z). Dashed lines: observed coal ranks (Fig. 2).

1) Effects of radiogenic heat production are negligible compared with cooling magma effects.
2) Latent heat effects can be simplified by adding 300° C to the initial intrusion temperature, if the coal is remote from the magma.
3) Lateral and vertical variations in rock properties have negligible influence on coalification compared to cooling magma effects, so a homogeneous medium is allowed.

These three conclusions justify the simplifications used in the 3D modeling.

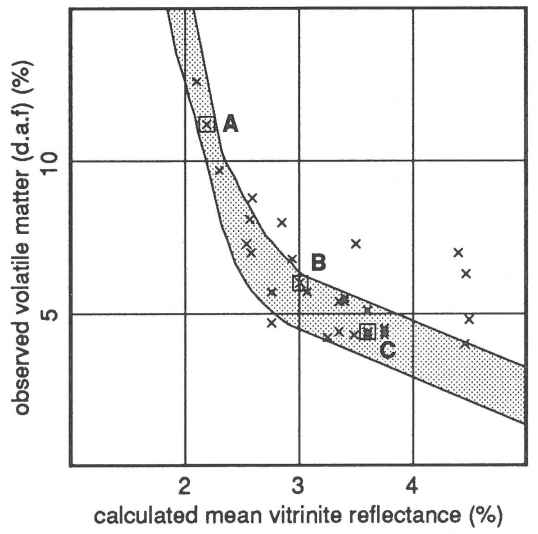

Fig. 11. Calculated vs. observed coal rank data for seam Steinknipp (Z). Shaded: expected relationship of Fig. 5. A B C as in Fig. 1.

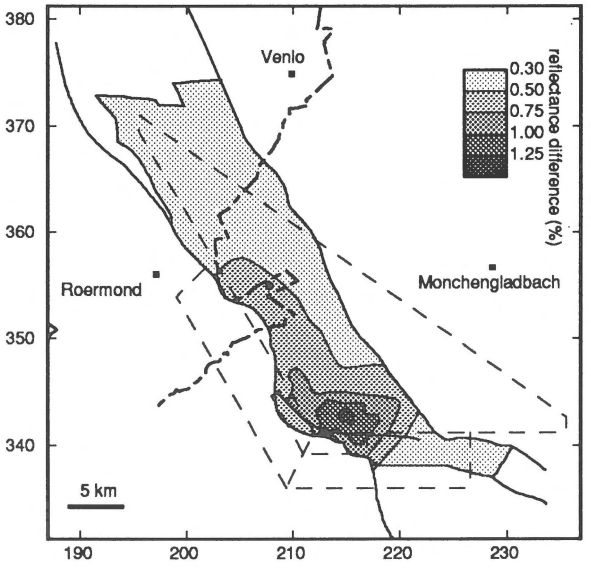

Fig. 12. Contour map of vertical differences in calculated reflectance (seam Z minus seam E). The vertical distance between seam Z and E is taken 370 m. Dashed lines: intrusion boundary of Bosum (1965).

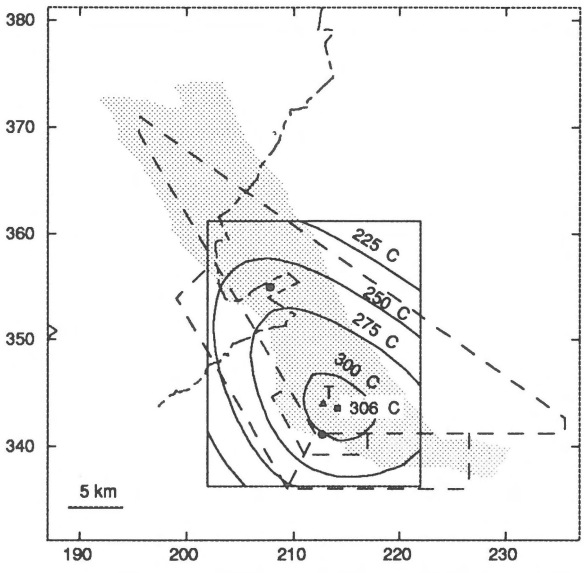

Fig. 13. Contour map of calculated maximum temperatures at restored geometry. Present level – 500 m Sophia-Jacoba 1. At point T a temperature of at least 204° C occurred.

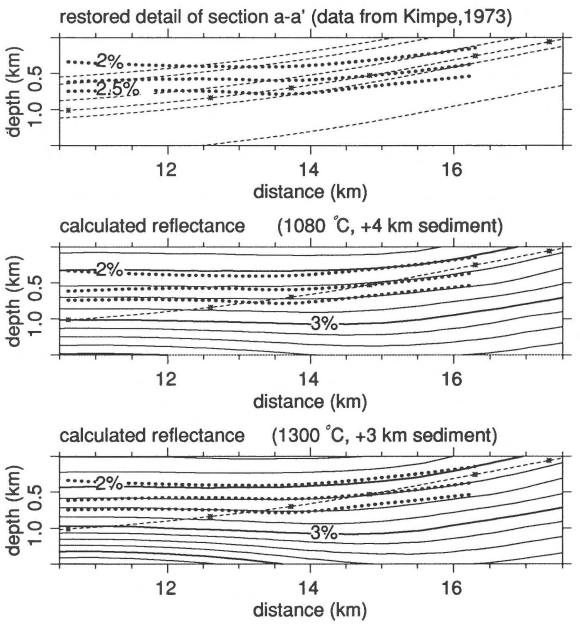

Fig. 14. Calculated 2D finite difference coal ranks for detail of section a-a′: section III of Kimpe (1973) (see Fig. 8). Numbers indicate reflectance. Solid lines: calculations; dotted lines: observed coal ranks; dashed lines: coal seams of Table 2; dashed line with stars: seam Steinknipp (Z).

Discussion

With the 3D modeling we found an initial intrusion temperature of (800 ± 100) °C. This rather low temperature agrees better with a felsic than with a mafic magma. A felsic intrusion, however, on this specific location on the outer fringe of the Variscan Orogen is very difficult to explain, because felsic magma is generated in the extreme conditions prevailing in the nucleus of an orogen. However, an example of a small anorogenic felsic intrusion (Jurassic) exists in the Zuidwal gas field in the north of the Netherlands (Perrot & Van der Poel 1987).

An alternative could be a mafic dyke-swarm intrusion within the Bosum (1965) geometry where the initial (high) temperature is averaged also over the enclosed country rock. This alternative is also favoured by V. Wrede and M. Teichmüller (pers. comm.).

A smaller igneous body with a stronger magnetisation could yield also the observed magnetic anomaly. The initial temperature at which this smaller body started to cool could then be higher. However, the density limitations found by Bredewout (1989) still have to be taken into account if a mafic composition is chosen.

To summarise; a felsic intrusion yields geological difficulties; a mafic intrusion yields geophysical difficulties.

Conclusions

It can be conclusively stated that the best fit on the observed data is obtained in 3D modeling with initial intrusion temperatures of about 1100° C. This temperature corresponds – after correcting for latent heat effects by subtracting a traditional 300° C – with an initial intrusion temperature of (800 ± 100) ° C. This rather low temperature agrees better with a felsic than with a mafic magma.

Calculated vertical coal rank gradients are comparable with those observed in the Ibbenbüren coalfield (Bramsche intrusion, FRG).

A 2D finite difference calculation using the complete heat equation on a detailed section in the area proved that

1) effects of radiogenic heat production are negligible compared to cooling magma effects;
2) latent heat effects can be simplified by adding 300° C to the initial intrusion temperature, if the coal is remote from the magma;
3) lateral and vertical variations in rock properties have negligible influence on coalification compared to cooling magma effects, so a homogeneous medium is allowed.

The results are important in two respects:

1: Local. The calculations have proven that a cooling magmatic body can explain the coalification anomaly of the Peel-Erkelenz coalfield.
2: General. 'Kitchening' model calculations are an inexpensive tool in the discovery process of anthracite, gas and oil fields in areas of magnetic anomalies caused by intrusions.

Acknowledgements

Hans Erren thanks Sierd Cloetingh for some helpful suggestions, Jilles van den Beukel for providing the initial finite difference software and Colin Reeves for correcting the text.

References

Bosum, W. 1965 Interpretation magnetischer Anomalien durch dreidimensionale Modellkörper zur Klärung geologischer Probleme – Geol. Jb. 83: 668–680

Bredewout, J.W. 1989 The character of the Erkelenz intrusive as derived from geophysical data – Geol. Mijnbouw 68: 445–454

Buntebarth, G. 1984 Geothermics, an introduction – Springer (Berlin): 144 pp

Buntebarth, G. 1985 Das Temperaturgefälle im Dach des Bramscher Massivs aufgrund von Inkohlungsuntersuchungen im Karbon von Ibbenbüren – Fortschr. Geol. Rheinld. Westf. 33: 255–264

Carslaw, H.S. & J.C. Jaeger 1962 Conduction of heat in solids. 2nd ed. – Clarendon Press (Oxford): 510 pp

Falvey, D.A. & I. Deighton 1982 Recent advances in burial and thermal geohistory analysis – APEA J. 22: 65–81

Giberti, G., S. Moreno & G. Sartoris 1984 Evaluation of approximations in modeling the cooling of magmatic bodies – J. Volc. Geoth. Res. 20: 297–310

Haenel, R. 1983 Geothermal investigations in the Rhenish Massif. In: K. Fuchs, K. Von Gehlen, H. Mälzer, H. Murawski & A. Semmel (eds): Plateau uplift, the Rhenish Shield, a case history – Springer (Berlin): 228–246

Horváth, F., P. Dövényi & I. Laczó 1986 Geothermal effect of magmatism and its contribution to the maturation of organic matter in sedimentary basins. In: G. Buntebarth & L. Stegena (eds): Lecture notes in Earth Sciences, 5, Paleogeothermics – Springer (Berlin): 173–183

Kimpe, W.F.M. 1973 The geology of the Carboniferous in the coal field Beatrix in Central Limburg, The Netherlands and in the adjacent German Area – Verh. Kon. Ned. Geol. Mijnbouwk. Gen. 29: 19–36

Patteisky, K., M. Teichmüller & R. Teichmüller 1962 Das Inkohlungsbild des Steinkohlengebirges an Rhein und Ruhr, dargestellt im Niveau von Flöz Sonnenschein – Fortschr. Geol. Rheinld. Westf. 3: 687–700

Peelcommissie 1963 Rapport van de Peelcommissie – Verh. Kon. Ned. Geol. Mijnbouwk. Gen., Mijnb. Ser. 5: 133 pp + maps

Perrot, J. & A.B. Van der Poel 1987 Zuidwal, a Neocomian gas field. In: J. Brooks & K. Glennie (eds): Petroleum geology of North West Europe – Graham & Trotman (London): 325–335

Teichmüller, M. 1987 Recent advances in coalification studies and their application to geology. In: A.C. Scott (ed.): Coal and coal-bearing strata: Recent Advances – Geol. Soc. Spec. Publ. 32: 127–169

Teichmüller, M. & R. Teichmüller 1966 Die Inkohlung des Saar-Lothringer Karbon, verglichen mit der im Ruhrkarbon – Dtsch. Geol. Ges. Z. 117: 243–279

Teichmüller, M. & R. Teichmüller 1984 Verbreitung und Eigenschaften tiefliegender Steinkohlen in der Bundesrepublik Deutschland – Glückauf Forschungshefte 45: H. 3

Teichmüller, M. & R. Teichmüller 1985 Inkohlungsgradienten in der Anthrazitfolge des Ibenbürener Karbons – Fortschr. Geol. Rheinld. Westf. 33: 231–253

Tissot, B.P., R. Pelet & Ph. Ungerer 1987 Thermal history of sedimentary basins, maturation indices, and kinetics of oil and gas generation – Am. Assoc. Pet. Geol. Bull. 71: 1445–1466

Van den Beukel, J. & R. Wortel 1986 Thermal modeling of arc-trench regions – Geol. Mijnbouw 65: 133–143

Van Tongeren, P.C.H. 1987 Renewed interest in coal. In: W.A. Visser, J.I.S. Zonneveld, A.J. van Loon (eds): Seventy-five years of geology and mining in the Netherlands (1912–1987) – Kon. Ned. Geol. Mijnbouwk. Gen. (The Hague): 231–242

Verwer, J.G. 1977 A class of stabilized three-step Runge-Kutta methods for the numerical integration of parabolic equations – J. Comp. Appl. Math. 3: 155–166

Wrede, V. 1985 Tiefentektonik des Aachen-Erkelenzer Steinkohlengebietes. In: G. Drozdewski, H. Engel, R. Wolf & V. Wrede (eds): Beiträge zur Tiefentektonik westdeutscher Steinkohlenlagerstätten – Geol. Landesamt Nordrhein-Westfalen, (Krefeld): 16–31 + maps